Dynamical network model of infective mobile agents

Mattia Frasca,[1,*] Arturo Buscarino,[1] Alessandro Rizzo,[2] Luigi Fortuna,[1] and Stefano Boccaletti[3]
[1]*Dipartimento di Ingegneria Elettrica Elettronica e dei Sistemi, Università degli Studi di Catania, viale A. Doria 6, 95125 Catania, Italy*
[2]*Dipartimento di Elettrotecnica ed Elettronica, Politecnico di Bari, Via Re David 200, 70125 Bari, Italy*
[3]*CNR-Istituto dei Sistemi Complessi, Via Madonna del Piano, 10, 50019 Sesto Fiorentino, Florence, Italy*
(Received 11 April 2006; published 21 September 2006)

A dynamical network (consisting of a time-evolving wiring of interactions among a group of random walkers) is introduced to model the spread of an infectious disease in a population of mobile individuals. We investigate the main properties of this model, and show that peculiar features arise when individuals are allowed to perform long-distance jumps. Such peculiarities are captured and conveniently quantified by a series of appropriate parameters able to highlight the structural differences emerging in the networks when long-distance jumps are combined with local random walk processes.

DOI: 10.1103/PhysRevE.74.036110 PACS number(s): 89.75.Fb, 05.65.+b

I. INTRODUCTION

Among the most studied models for investigating the spread of infectious diseases, the well-known susceptible-infected-susceptible (SIS) and susceptible-infected-recovered (SIR) models have attracted considerable attention since their introduction [1,2]. These models are described by two and three coupled ordinary differential equations, respectively, where the state variables correspond to the number of susceptible (S) and infected (I) individuals in the SIS model; and to that of susceptible (S), infected (I), and recovered (R) individuals in the SIR model. The two models account for two different types of infectious diseases: in the case of the SIR model a long-life immunity is gained after the recovering from the infection, while repeated infections can occur for the same individual in the SIS model. Both models reproduce the spread of a disease in a population of N individuals, under idealized hypotheses, such as that all the individuals have the same kind of response to the disease and that the population mixes at random (i.e., all the individuals have the same probability of contacting the other individuals).

These models have been extended in many ways, for example, to study the disease spread in a population divided into subgroups which may influence each other (for instance, the case of a disease spreading from city to city by means of travellers [3]). Other extensions have been considered, and a great source of inspiration to mathematical epidemiology has been recently provided by network theory and its advances. In particular, the studies on complex networks have provided mathematical epidemiology with new ideas and tools which have led to models in which the structure of interactions between individuals is taken into account. Social connections can, indeed, be mapped into idealized network structures, replicating the structure underlying real data (for a review on the topic of networks and epidemic models see Ref. [4]; for a recent review on complex networks see Ref. [5]). Recent studies show that in many cases the resulting networks display the presence of interconnected individuals with large number of contacts (scale-free networks [5]) and highlight their key role in disease spread and vaccination policies [4]. In particular, a very interesting property emerging in the study of such scale-free networks is that the epidemic threshold (a critical value of the parameters such that no infinite epidemic can occur if they are under these values) vanishes exactly [6–8]. Recently, the case of two pathogens in a single population whose contacts are modelled by scale-free networks has been investigated in Ref. [9]. Models based on scale-free and small-world networks have been also applied to concrete studies on the transmission of recent diseases such as SARS [10]. For instance, Hufnagel *et al.* [11] implement a very detailed probabilistic model of transmission and recovery dynamics, in which local dynamics of disease occurring in urban communities can affect each other by means of a global connection network, based on real data, able to emulate the civil aviation traffic.

Most of the studies presented so far concern the case of static networks, i.e., wiring structures of connections between individuals that are given (or grown) once forever, and that are taken as fixed in time. In the case of disease dynamics, this means that the social interaction structure is fixed in time and space. In this paper, instead, we explicitly consider the case of dynamical networks, i.e., wirings for which the connections between individuals are let to evolve in time. Through the paradigm of dynamical networks, this study tries to parallel a realistic case in which people are allowed to move, and consequently the connection structure changes. Precisely, the individuals constituting the nodes of the graph are here random walkers, which may additionally perform long-distance jumps and, similarly to the case of Refs. [12,13], are only able to interact with individuals falling within a given interaction radius apart from them. It must be mentioned at this stage that mobile agents were also considered in Ref. [14], where however the system was modelled by molecular dynamics and the only case of the SIS model was investigated.

II. THE MODEL

Let us consider N individuals distributed in a planar space, and let $\mathbf{v}_i(t)$ and $\theta_i(t)$ be the velocity and the direction

*Electronic address: mfrasca@diees.unict.it

of motion of the ith spreading agent $[\mathbf{v}_i(t) \equiv (v \cos \theta_i(t), v \sin \theta_i(t))$, v being the modulus of the agent velocity, which is the same for all individuals]. In our model, the agents are random walkers that update stochastically the direction angle $\theta_i(t)$. The position and the orientation of each particle are updated according to

$$\mathbf{x}_i(t + \Delta t) = \mathbf{x}_i(t) + \mathbf{v}_i(t)\Delta t,$$

$$\theta_i(t + \Delta t) = \xi_i(t + \Delta t), \tag{1}$$

where $\mathbf{x}_i(t)$ is the position of the ith particle in the plane at time t, and $\xi_i(t)$ are N independent random variables chosen at each time with uniform probability in the interval $[-\pi, \pi]$. In addition, to include the possibility that individuals can move through the bidimensional world with time constants much shorter than those related to disease, as in the case of infected individuals travelling by flight, we consider the case that individuals may perform long-distance jumps. This is accounted for by defining a parameter p_{jump} that quantifies the probability for an individual to perform a long-distance jump. In summary, at each time step, each agent evolves following Eqs. (1) [with $\mathbf{v}_i(t) = (v \cos \theta_i(t), v \sin \theta_i(t))$] with probability $1 - p_{\text{jump}}$ or performs a jump with probability p_{jump}. In this case Eqs. (1) with $\mathbf{v}_i(t) = (v_M \cos \theta_i(t), v_M \sin \theta_i(t))$, where $\frac{v}{v_M} = 0.03$, are used. In this way, an agent can make a long-distance jump into a random position, far from its previous position. In the following, the model is investigated as a function of the parameter p_{jump}, starting from the case in which the agents are pure random walkers ($p_{\text{jump}} = 0$) and extending it to the case of allowed random jumps ($p_{\text{jump}} \neq 0$).

Like traditional SIR models, each agent has three states: susceptible (S), infected (I), and recovered (R). A given number of individuals is taken at $t = 0$ as the seed of the infection ($I_0\% = 2\%$), while all the others start from the susceptible state. The process through which the infection spreads can be summarized as follows: an interaction radius r is defined, such that each agent interacts at a given time with only those agents located within a neighborhood of radius r. For a given agent, the probability of being infected increases with the number of infected individuals in the neighborhood. More precisely, if an agent is in the S state at time t, and exactly one of its neighbors is in the I state, then it moves into the I state with probability p_{inf}, and stays in the S state with probability $1 - p_{\text{inf}}$. If N_{I_r} is the number of infected individuals in the neighborhood of the agent, then its probability of being infected is $p_{\text{cont}} = 1 - (1 - p_{\text{inf}})^{N_{I_r}}$. We further suppose that the infection lasts τ simulation steps, so that all infected individuals become recovered τ simulation steps after having assumed the I state and, after that time, they cannot catch the disease anymore. The size of the plane where individuals move is L (that, from here on, will be measured in units of the radius r), and periodic boundary conditions are considered.

III. RESULTS

Model (1) predicts that the disease spreads with an evolution which resembles that predicted by classical SIR models. The model is simulated for T steps with $\Delta t = 1$ (arbitrary time units). In all the simulations considered in this paper this parameter is fixed to $T = 150$, which is sufficiently high to ensure that after T steps the disease disappears, since there are no more infected individuals in the population. During a simulation, the number of infected grows up, reaches a peak value, and then decreases. A typical case is shown in Fig. 1, where it can be noticed that at the end of the simulation not all the individuals have been infected: in fact, there is a residual percentage of susceptible individuals that cannot contract the disease, since all infected individuals have been recovered. The model also predicts that long-distance jumps increase the spread of the infection: in presence of long-distance jumps the maximum number of infected individuals (defined as $I_{\max}$) and the number of individuals which have contracted the disease at the end of the simulation (defined as $R_{\max}$) are higher. Both the two issues have important consequences, since on one hand the disease involves a higher percentage of the population, and, on the other hand, it requires more resources to deal with a higher peak of infected individuals.

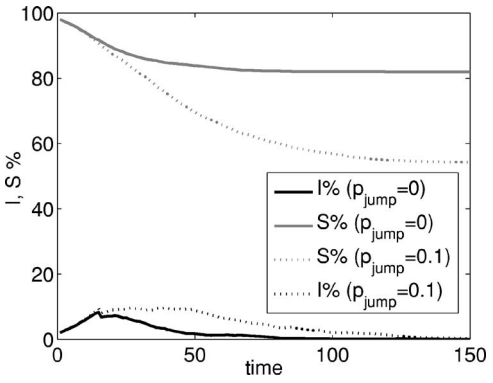

FIG. 1. Evolution of the percentage of susceptible and infected individuals in Eq. (1) with $p_{\text{jump}} = 0$ (continuous lines) and $p_{\text{jump}} = 0.1$ (dotted lines). The other parameters are $N = 200$, $v = 0.03$, $\rho = 1$, $I_0\% = 2\%$, $\tau = 15$, $p_{\text{inf}} = 0.05$. Results are averaged over 20 runs.

The effects of long-range jumps are similar to those of long-range connections investigated in Ref. [4], where it is shown that small-world networks compared to the case of local interaction networks have more virulent infections. The reason is that small-world networks combine two important factors in disease spread: a high level of clustering, which implies that the infection mostly spread on a local basis, and a lower characteristic path length, which accounts for a rapid epidemic spread, even towards groups located far from the infected clusters [15].

The behavior of model (1) was also characterized with respect to different values of the density of individuals, i.e., $\rho = \frac{N}{L^2}$. As it may be intuitively expected, as the density increases, more individuals contract the disease. The maximum percentage of infected and recovered individuals at the end of the simulation increase when density increases, as shown in Fig. 2. As can be noticed, the curves related to the case with $p_{\text{jump}} = 0.1$ are always above those related to the case with $p_{\text{jump}} = 0$. This allows us to conclude that the introduction of long-distance jumps ($p_{\text{jump}} = 0.1$) lets the infection

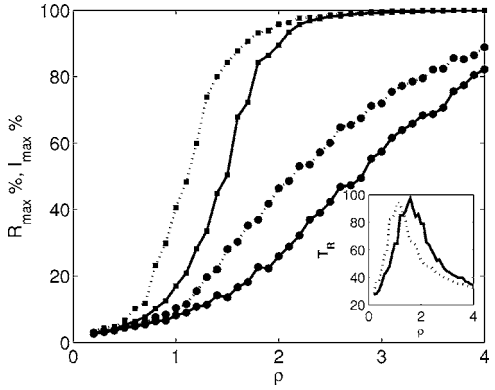

FIG. 2. Maximum percentage of infected (●, circles) and recovered (■, squares) individuals with respect to density ρ in the case $p_{\text{jump}}=0$ (continuous lines) and $p_{\text{jump}}=0.1$ (dotted lines). In the inset the trend of T_R vs ρ is shown. The other parameters of the model are $N=200$, $v=0.03$, $I_0\%=2\%$, $\tau=15$, $p_{\text{inf}}=0.05$. Results are averaged over 40 runs.

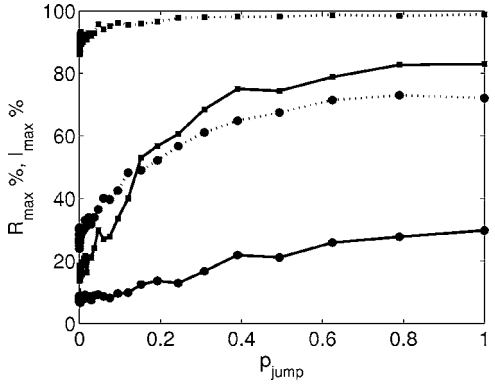

FIG. 3. Behavior of the model with respect to p_{jump}. The maximum percentage number of infected (●, circles) and recovered (■, squares) individuals versus p_{jump} for two different values of ρ are shown: $\rho=1$ (continuous line) and $\rho=2$ (dotted line). The parameters of the model are $N=200$, $v=0.03$, $I_0\%=2\%$, $\tau=15$, $p_{\text{inf}}=0.05$. Results are averaged over 20 runs.

spread on a larger percentage of individuals at any density.

For an accurate characterization of the model, it is also important to evaluate the velocity with which the disease spreads. To this aim, the time needed to reach the 90% of the final value of the number of recovered individuals, defined as T_R, is evaluated. This characteristic time is evaluated for different values of the density ρ. Results are shown in Fig. 2, where the trend of T_R versus ρ is illustrated. It can be noted that both reported curves (for $p_{\text{jump}}=0$ and $p_{\text{jump}}=0.1$) exhibit a peak. This is due to the fact that increasing the density leads to two opposite effects: for large values of the density the disease spread is faster; on the contrary, when density is low, a lower number of individuals contract the infection. In the case of long-distance jumps, the peak is located at lower density values. Thus, long-distance jumps have the effect of increasing T_R for low density values, since a larger population is involved in the disease. On the other hand, for high density values, T_R decreases in presence of long-distance jumps, since the disease spread is faster.

A further characterization of model (1) refers to the behavior with respect to different values of p_{jump}. The maximum percentage of infected and recovered individuals is evaluated for different values of p_{jump}. Moreover, two different values of the density ρ ($\rho=1$ and $\rho=2$) are considered. The results, shown in Fig. 3, reveal that the number of individuals which have contracted the infection grows as p_{jump} is increased. The number of recovered individuals at the end of the simulation and the maximum percentage of infected individuals with density $\rho=2$ are higher than in the case with $\rho=1$.

After a qualitative analysis of system behavior, adequate parameters able to characterize and explain the system behavior are searched for. Since the system investigated in this paper can be characterized by the network of interactions between individuals, we first looked at the characteristics of this network. This network has links which evolve in time and thus, according to the definition discussed in Ref. [5], it is a *dynamical* network. Dynamical networks arise in a large variety of phenomena, but there is no standard way to characterize their properties. The definition of clustering coefficient C, characteristic path length L and mean node degree $\langle k\rangle$ can be adapted from the theory of networks with static links [5], and in this case time-dependent parameters arise. We calculated these parameters, but despite the evident differences of the epidemic behavior in the cases $p_{\text{jump}}=0$ and $p_{\text{jump}}=0.1$ previously shown, these parameters do not show significant differences, as illustrated in Fig. 4. The conclusion is that other parameters should be used to characterize the model.

The definition of the new parameters was inspired by the following considerations connected to the nature of the investigated model. Each infected individual may infect other individuals during the whole duration of its infection (i.e., during τ simulation steps). Therefore, each individual may infect others if they are within its interaction radius at a given time t, but also if other individuals are within its interaction radius at the simulation steps $t+1,\ldots,t+\tau-1$. For this reason, a new interaction network should be defined. Let $A(t)$ be the interaction network at time t. This matrix is defined as an adjacency matrix, in which $a_{ij}(t)=1$ if the jth agent is

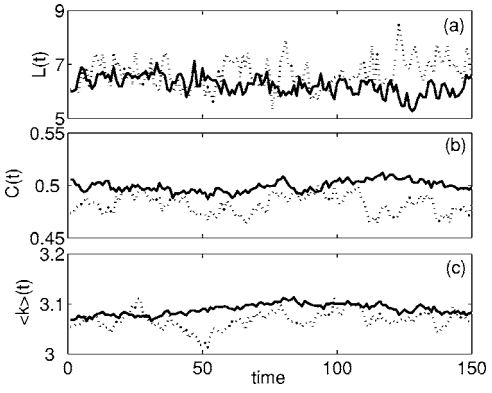

FIG. 4. $L(t)$, $C(t)$, and $\langle k\rangle(t)$ for the two cases $p_{\text{jump}}=0$ (continuous lines) and $p_{\text{jump}}=0.1$ (dotted lines). The parameters of the model are $N=200$, $v=0.03$, $\rho=1$, $I_0\%=2\%$, $\tau=15$, $p_{\text{inf}}=0.05$. Results are averaged over 20 runs.

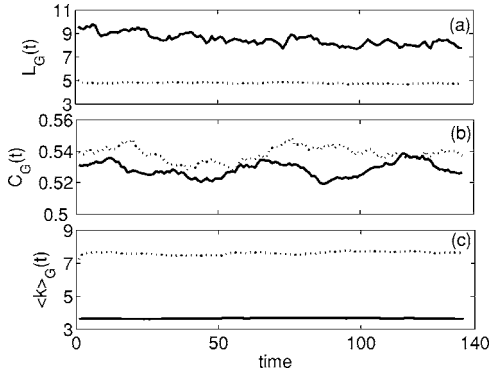

FIG. 5. $L_G(t)$, $C_G(t)$, and $\langle k\rangle_G(t)$ for $p_{\text{jump}}=0$ (continuous lines) and $p_{\text{jump}}=0.1$ (dotted lines). The parameters of the model are $N=200$, $v=0.03$, $\rho=1$, $I_0\%=2\%$, $\tau=15$, $p_{\text{inf}}=0.05$. Results are averaged over 20 runs.

within the interaction radius of the ith agent at time t, and $a_{ij}(t)=0$ otherwise [furthermore, it is assumed that $a_{ii}(t)=1$, $\forall i=1,\ldots,N$]. The new interaction network accounting for contacts occurring during the whole infection period is defined as $G(t)$ for $t=1,\ldots,T-\tau+1$ where $g_{ij}(t)=1$ if at least for one k (with $k=t,\ldots,t+\tau-1$) it is verified that $a_{ij}(k)=1$; $g_{ij}(t)=0$ otherwise.

The new interaction graph, defined through the $G(t)$ interaction matrix, is characterized by calculating the clustering coefficient $C_G(t)$, the characteristic path length $L_G(t)$ and the mean node degree $\langle k\rangle_G(t)$. The results are shown in Fig. 5, in which can be clearly noted that traditional graph parameters, evaluated on the newly defined interaction matrix, can effectively characterize the differences of the epidemic behavior shown by the two investigated cases. $L_G(t)$ and $\langle k\rangle_G(t)$ oscillate around a (temporal) mean which is totally different in the two cases. In particular, it is clear that the network with $p_{\text{jump}}=0.1$ has a higher mean node degree $\langle k\rangle_G(t)$ and a lower characteristic path length $L_G(t)$ with respect to the case with $p_{\text{jump}}=0$. The different values of these two parameters explain why the infection is more virulent in the case with $p_{\text{jump}}=0.1$. The mean value of $L_G(t)$ when $p_{\text{jump}}=0.1$ is lower than that obtained when $p_{\text{jump}}=0$; this explains why the infection can reach the individuals of the population more easily. Similarly, since the time average of $\langle k\rangle_G(t)$ is higher when $p_{\text{jump}}=0.1$, mobile agents have more potentially infectious contacts with other individuals when they are allowed to make long-distance jumps.

The behavior of the model with respect to different values of the density ρ is now characterized in terms of the new parameters introduced, namely $L_G(t)$ and $\langle k\rangle_G(t)$. The results are shown in Fig. 6, where for the sake of simplicity only the values of $L_G(t)$ and $\langle k\rangle_G(t)$ at the end of the simulation (i.e., at $t=t_f=T-\tau+1$) are considered. The mean node degree $\langle k\rangle_G(t_f)$ versus ρ is monotonic; in fact, as intuition suggests, individuals in populations with higher density are more connected to each other. On the other hand, the characteristic path length has a peak and then decreases. When compared with the characterization of the model in terms of the time T_R (shown in the inset of Fig. 2), this result leads to the conclusion that, at least qualitatively, the trend of $L_G(t_f)$ versus ρ

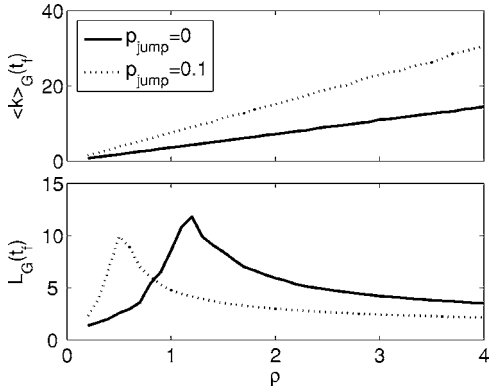

FIG. 6. $\langle k\rangle_G(t_f)$ and $L_G(t_f)$ versus ρ for two different values of p_{jump}: $p_{\text{jump}}=0$ (continuous line) and $p_{\text{jump}}=0.1$ (dotted line). The parameters of the model are $N=200$, $v=0.03$, $I_0\%=2\%$, $\tau=15$, $p_{\text{inf}}=0.05$. Results are averaged over 20 runs.

can explain the behavior of T_R. Similarly, the monotonous trend shown by the maximum percentage of infected individuals versus ρ (Fig. 2) seems more influenced by the mean node degree than by the characteristic path length of the interaction network. Namely, the analysis of the dependence of $I_{\max}$ vs $\langle k\rangle_G$ shows that a cubic polynomial fits very well the data. On the other side, fitting the data of T_R vs L_G is a rather difficult task, as the data are quite irregular.

The parameters $L_G(t)$ and $\langle k\rangle_G(t)$ are also evaluated with respect to different values of the transport parameter p_{jump}. Results are shown in Fig. 7. The curve $L_G(t_f)$ versus p_{jump} reveals a strong similarity with that illustrating the dependence of the synchronization thresholds on the probability parameter in the so-called blinking model [16]. The blinking model is a dynamical small-world network in which long-range connections between any pair of network nodes can be activated with a given probability for a given period. Therefore, the whole network has links which change over time according to a given probability. The characterization of the synchronization thresholds shows a similar functional dependence on the probability parameter. Since the characteristic

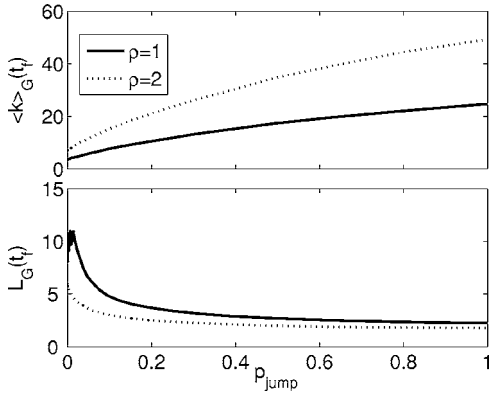

FIG. 7. Behavior of the model with respect to p_{jump}. $L_G(t_f)$ and $\langle k\rangle_G(t_f)$ vs p_{jump} for two different values of ρ: $\rho=1$ (continuous line) and $\rho=2$ (dotted line). The parameters of the model are $N=200$, $v=0.03$, $I_0\%=2\%$, $\tau=15$, $p_{\text{inf}}=0.05$. Results are averaged over 20 runs.

path length is connected with synchronization properties of a network, this similarity is not surprising and it is reasonable to state that this kind of behavior is common to dynamical networks with links which evolve according to a random process.

Disease control strategies related to the proposed model are now discussed. The proposed model shares with the model by Hufnagel *et al.* [11] the advantage of adopting a microscopic description of the moving individuals. This suggests new strategies to inhibit the disease spreading, and, in particular, it suggests to impose movement restrictions to control the disease spreading. As the behavior of $R_{\max}$ and $I_{\max}$ versus p_{jump} (Fig. 3) and that of L_G and $\langle k\rangle_G$ (Fig. 7) show, a trivial strategy to inhibit the infectious spread is to reduce p_{jump}. Furthermore, in the framework of the microscopic description of individual motion, a new strategy can be defined: to inhibit long-range movements (i.e., the jumps) of infected individuals. We simulated this case and we obtained that, by using this strategy (with $p_{\text{jump}}=0.1$), $R_{\max}$ and $I_{\max}$ are almost identical to those of the case with $p_{\text{jump}}=0$. Thus, adopting this strategy is effective to reduce the number of recovered and infected individuals. On the other hand, the parameters L_G and $\langle k\rangle_G$ represent the characteristic of agent motion, and therefore are able to explain the mechanism of disease spreading when the disease can effectively spread on the basis of the agent movements. When infected individuals are not allowed to perform long-range jumps, one expects that on average the motion characteristics are similar to the case in which infected individuals may perform long-range jumps, but disease spreading is reduced. Simulation results (not shown) in the case with disease control and $p_{\text{jump}}=0.1$, confirmed that $R_{\max}$ and $I_{\max}$ are similar to the case without disease control and with $p_{\text{jump}}=0$, and L_G and $\langle k\rangle_G$ are similar to the case without disease control and $p_{\text{jump}}=0.1$. Thus, this strategy reduces the number of infected individuals without significant modifications of the agent motion characteristics.

IV. CONCLUSIONS

In this paper a model of infective mobile agents is introduced. The model is investigated under the perspective of the dynamical network underlying the time-evolving interactions between the agents. The agents are random-walkers which, additionally, may perform long-distance jumps with a given probability. Therefore the movement of the walkers is a random superposition of two walks of the same kind, each with a different time scale. In these random walks the direction of the movement is uniformly distributed while the module of the velocity is constant. The case in which the module of the velocity v_M of the second random walk is not constant has been also investigated. Several probability distribution functions for v_M were considered: one with v_M taken from an uniform distribution and another one with v_M taken from a power-law distribution with exponent $\gamma=2$. In both cases the obtained results were intermediate between the two reported cases. Therefore, the results seem independent on the implementation of the second random walk.

We showed that a straightforward generalization of the parameters characteristic of static networks (i.e., the evaluation of instantaneous values of characteristic path length, mean node degree and clustering coefficient) to the time-dependent case does not reveal the differences which are clearly evident by the analysis of disease spreading with $p_{\text{jump}}=0$ and $p_{\text{jump}}\neq 0$. However, if the key features of the infective process are taken into account in the definition of a new matrix of interactions, $G(t)$, the characteristic path length and the mean node degree calculated on $G(t)$ are able to explain the differences between the two cases. Furthermore, the dependence of the characteristic path length of $G(t)$ on the probability of jump is similar to that observed in other dynamical networks with links evolved according to a random process.

ACKNOWLEDGMENTS

This work was partially supported by the Italian "Ministero dell'Istruzione, dell'Università e della Ricerca" (MIUR) under the projects Firb RBNE01CW3M and by the EU under COST ACTION B27 ENOC. One of the authors (S.B.) acknowledges the Yeshaya Horowitz Association through the Center for Complexity Science.

[1] W. Kermack and A. McKendrick, Proc. R. Soc. London, Ser. A **115**, 700 (1927).
[2] H. Hethcote, SIAM Rev. **42**, 599 (2000).
[3] P. Ogren and C. F. Martin, Proceedings of the 39th Conference on decision and control, 2000, pp. 1782–1787.
[4] M. Keeling and K. Eames, J. R. Soc., Interface **2**, 295 (2005).
[5] S. Boccaletti, V. Latora, Y. Moreno, M. Chavez, and D.-U. Hwang, Phys. Rep. **424**, 175 (2006).
[6] R. Pastor-Satorras and A. Vespignani, Phys. Rev. E **63**, 066117 (2001).
[7] Y. Moreno, R. Pastor-Satorras, and A. Vespignani, Eur. Phys. J. B **26**, 521 (2002).
[8] M. E. J. Newman, Phys. Rev. E **66**, 016128 (2002).
[9] M. E. J. Newman, Phys. Rev. Lett. **95**, 108701 (2005).
[10] M. Small and C. K. Tse, Int. J. Bifurcation Chaos Appl. Sci. Eng. **15**, 1745 (2005).
[11] L. Hufnagel, D. Brockmann, and T. Geisel, Proc. Natl. Acad. Sci. U.S.A. **101**, 15124 (2004).
[12] A. Buscarino, L. Fortuna, M. Frasca, and A. Rizzo, Chaos **16**, 015116 (2006).
[13] T. Vicsek, A. Czirok, E. Ben-Jacob, I. Cohen, and O. Shochet, Phys. Rev. Lett. **75**, 1226 (1995).
[14] M. Gonzalez and H. J. Herrmann, Physica A **340**, 741 (2004).
[15] D. Watts and S. H. Strogatz, Nature (London) **393**, 440 (1998).
[16] I. V. Belykh, V. N. Belykh, and M. Hasler, Physica D **195**, 188206 (2004).